Lift Control of Electric Airplanes by Using Propeller Slipstream for Safe Landing

Nobukatsu Konishi, Hiroshi Fujimoto,
Yasumasa Watanabe, and Kojiro Suzuki
The University of Tokyo
5-1-5, Kashiwanoha, Kashiwa, Chiba, 227-8561 Japan
Phone: +81-4-7136-3881
Email: konishi@hflab.k.u-tokyo.ac.jp, fujimoto@k.u-tokyo.ac.jp,
watanabe@daedalus.k.u-tokyo.ac.jp, kjsuzuki@k.u-tokyo.ac.jp

Hiroshi Kobayashi and Akira Nishizawa
Institute of Aeronautical Technology
Japan Aerospace Exploration Agency
6-13-1, Osawa, Chofu-shi, Tokyo, 181-0015 Japan
Phone: +81-50-3362-4458
Email: kobayashi.hiroshi2@jaxa.jp,
nishizawa.akira@jaxa.jp

***Abstract*—Aircrafts are desired to be more energy efficient and safer due to the increasing demand for air transportations. However, generally speaking, nowadays commercial airplanes tend to loss stability under wind disturbances, especially during landing. On the other hand, electric airplanes (EAs) are believed to satisfy the two demands because electric motors are used for the propulsion. Especially, as the actuators, electric motors can improve the control performances of EAs compared with internal combustion engines (ICEs). In this paper, by utilizing electric motors' advantages, lift control method using propeller slipstream is proposed for safe landing, which might be a key technology to innovate the design of EAs. Moreover, simulations and experiments are conducted to verify the effectiveness of the proposed method.**

I. Introduction

A. Background

Considering the increasing demand for air transportation, aircrafts are desired to be more energy efficient and safer. Electric airplanes (EAs) are believed to satisfy these demands due to the utilization of electric motors for propulsion [1]–[4]. Compared with internal combustion engines (ICEs), motors have the following remarkable advantages [5].

- Response of motor torque is much faster than that of internal combustion engines (over 100 times).
- Distributed installation and independent control are easy.
- Motor torque can be measured precisely from the current.
- The electric motors are more efficient than ICEs.

There are some studies [6] [7] on safety and efficiency control for EAs by utilizing these advantages and it is widely recognized that EAs will have multiple motors and propellers.

B. Objective

Although nowadays airplanes including EAs are designed to have higher stability and controllability, over 60 % accidents of light airplanes were occurred during approaching and landing [4] [8]. Besides, landing weight of EAs is larger than that of a normal airplane, because the weight of battery-powered EAs is not decreased during the flight. Solving this problem is challenging, and current works focus on making temporary lift. Some studies control a high lift device as a powered high-lift system [9] [10], and another has to employ plasma actuators [11]. These solutions, however, need extra devices to increase the weight and the response of these devices are not fast enough for safety improvement.

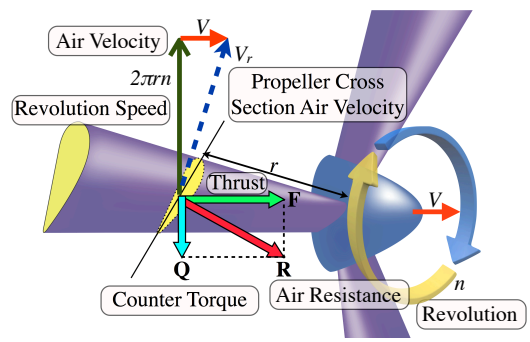

Fig. 1. Physics of propeller cross section.

In order to solve the problem, this paper proposes a lift control method that uses the propeller slipstream, and the fast response of motors can therefore be utilized.

II. Modeling of Multiple Propellers Electric Airplane

In this section, the dynamics for an airplane with multiple propellers is explained.

A. Propeller Dynamics

Figure 1 shows the cross section of a propeller blade at distance r from hub. During flying, the propeller cross section moves as a composition of rotation and forward motion. Therefore, the cross section moves as a spiral. Assume the airflow is parallel to the axis of propeller. Airspeed V_x is the relative velocity between the air and airplane. Counter torque R is generated by the blade of propeller, and R can be resolved into the direction of the motion of the airplane "thrust" F and the direction of propeller revolution "counter torque" Q. Assume the air density is ρ, the propeller whose diameter D_p rotates at the propeller revolution speed n, and generates the

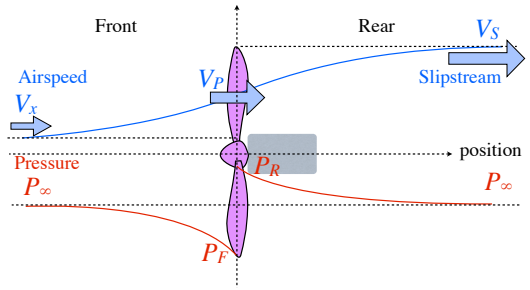

Fig. 2. Propeller slipstream diagram.

thrust F and the counter torque Q which can be express as

$$F = C_F(J)\rho n^2 {D_p}^4, \quad (1)$$
$$Q = C_Q(J)\rho n^2 {D_p}^5, \quad (2)$$

where C_F is propeller thrust coefficient, and C_Q is propeller counter-torque coefficient. Generally, each of them is a function of advance ratio J which is defined as

$$J = \frac{V_x}{nD_p}, \quad (3)$$

B. Propeller Slipstream

When a propeller rotates and generates thrust, propeller slipstream occurs and velocity of slipstream is amplified with respect to velocity of airspeed. Figure 2 illustrates the diagram between airspeed and propeller slipstream. V_x is airspeed, V_p is wind speed through propeller, and V_s is propeller slipstream. P_∞ is the pressure outside propeller stream, P_F is the pressure of the front face of propeller, and P_R is that of the rear face. Eq. (4) is realized from infinite direction ahead to the front face of the propeller, and Eq. (5) is realized from the rear dace of the propeller to infinite direction of back, based on Bernoulli's theorem.

$$\frac{1}{2}\rho {V_x}^2 + P_\infty = \frac{1}{2}\rho {V_p}^2 + P_F, \quad (4)$$
$$\frac{1}{2}\rho {V_p}^2 + P_R = \frac{1}{2}\rho {V_s}^2 + P_\infty. \quad (5)$$

Because thrust is basically the force on a propeller caused by the pressure difference between front face and rear face of the propeller, Eq. (6) is obtained as propeller thrust by multiplying the disk-area of the propeller and the pressure difference,

$$F = \frac{\pi}{4}{D_p}^2(P_R - P_F). \quad (6)$$

From Eq. (4) $\sim$ Eq. (6) are reformulated as Eq. (7).

$$\begin{aligned} F &= \frac{\pi}{4}{D_p}^2\frac{\rho}{2}({V_s}^2 - {V_x}^2) \\ &= \frac{\pi}{8}\rho {V_x}^2 {D_p}^2\left\{\left(\frac{V_s}{V_x}\right)^2 - 1\right\}. \end{aligned} \quad (7)$$

By reformulating Eq. 7, slipstream V_s is obtained as

$$V_s = V_x\sqrt{1 + \frac{8}{\pi}C_F(J)\left(\frac{nD_p}{V_x}\right)^2}. \quad (8)$$

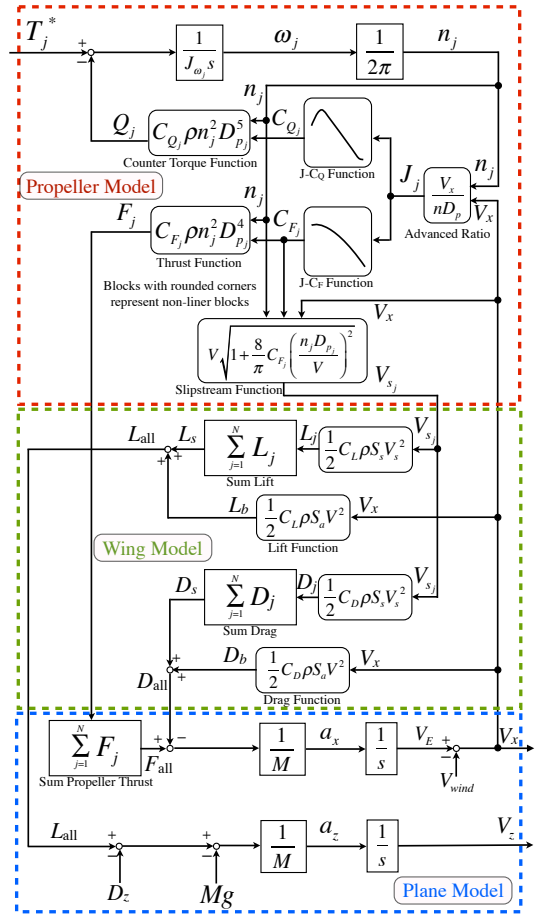

Fig. 3. Model block of plane with multiple propellers.

C. Aerodynamic Force of Wing

When an airplane has N propellers, some propellers are on the right wing, and the others are on the left wing, and the subscript j represents jth propeller. S is wing area, S_{s_j} is area which slipstream of a propeller blows against, and S_a is area which airspeed blows against. S can be expressed in short as

$$S = \sum_{j=1}^{N} S_{s_j} + S_a. \quad (9)$$

C_L is lift coefficient and C_D is drag coefficient. Total lift L_{all} is a summation of lift L_{s_j} by each propeller slipstream and lift L_a by airspeed as Eq. (10). In the same way, total drag D_{all} is a total of drag D_{s_j} by each propeller slipstream and drag D_a by airspeed as Eq. (11).

$$\begin{aligned} L_{\text{all}} &= \sum_{j=1}^{N} L_{s_j} + L_a \\ &= \frac{1}{2}\rho C_L \sum_{j=1}^{N} S_s {V_s}^2 + \frac{1}{2}\rho C_L S_a {V_x}^2, \end{aligned} \quad (10)$$

$$\begin{aligned} D_{\text{all}} &= \sum_{j=1}^{N} D_{s_j} + D_a \\ &= \frac{1}{2}\rho C_D \sum_{j=1}^{N} S_s {V_s}^2 + \frac{1}{2}\rho C_D S_a {V_x}^2. \end{aligned} \quad (11)$$

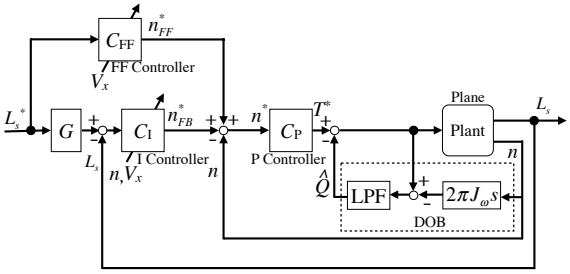

Fig. 4. Lift controller for each propeller.

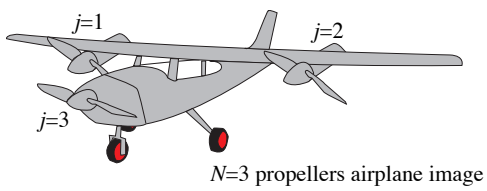

Fig. 5. Plane with 3 propellers

It is assumed that propeller slipstream are not interfered with each other and the slipstream speed V_{s_j} is spreaded over the slipstream area S_{s_j}.

D. Motion Equation of Plane

When the airplane with N propellers moves straight at airspeed V_x and accelerates at a_x and a_z, the equations of plane dynamics on horizon axis is expressed as Eq. (12) and the equation on vertical axis is expressed as Eq. (13).

$$Ma_x = F_{\text{all}} - D_x, \tag{12}$$

$$Ma_z = L_{\text{all}} - D_z - Mg. \tag{13}$$

The relationship among airspeed V_x, ground speed V_E, and a wind speed V_{wind} is Eq. (14).

$$V_x = V_E - V_{\text{wind}}. \tag{14}$$

The model of airplane with multiple propellers can be expressed as Fig. 3. In this paper, V_{wind} is ignored, and V_x is equal to V_E.

III. Designing of Lift Control of Multiple Propellers Electric Airplane

In this section, designing lift control by slipstream is explained as a proposed method. The controller has a disturbance observer (DOB) to compensate for propeller counter torque which is regarded as disturbance, a propeller revolution speed controller C_{P} at the inner loop, and a lift controller C_{I} at the outer loop.

A. Designing of Propeller Counter Torque Observer and Revolution Speed Controller

In this part, counter torque observer (CTO) and revolution controller are designed in a dotted line box on Fig. 4 by referring to [13].

The propeller counter torque can be expressed as

$$Q = T - 2\pi J_\omega \dot{n}. \tag{15}$$

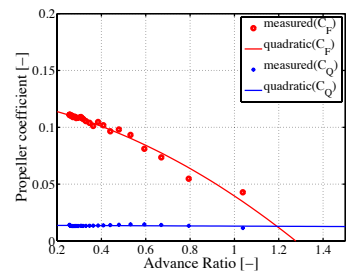

Fig. 6. Propeller characteristics.

TABLE I. Parameter in simulation.

air density ρ	1.23 kg/m^3
gross weight M	0.70 kg
wing area S	0.0963 m^2
lift coefficient C_L	1.014
drag coefficient C_D	0.149
propeller diameter D_p	254 mm
nominal propeller inertia J_ω	4.30×10^{-5}kg ·m
cut-off frequency ω_c	200 rad/s
proposed revolution controller pole ω_n	50 rad/s
conventional revolution controller pole ω_{conv}	0.4 rad/s
lift controller pole ω_{lift}	10 rad/s
reference model pole ω_g	50 rad/s

Therefore, if motor torque T and revolution speed n is detected, propeller counter torque $\hat{Q}$ can be estimated with a propeller counter torque observer as shown in a dotted line box on Fig. 4. In this paper, it is assumed that the current controller is adequately fast to use motor torque reference T^* for estimation, By adding the estimated value to the torque command, the plant is nominalized as Eq. (16) at frequency ranges below the cut-off frequency ω_{c} of the low pass filter of the CTO.

$$P_{\text{nom}} = \frac{1}{2\pi J_\omega s}. \tag{16}$$

The revolution speed control is done by proportional controller. The gain C_{P} of the controller is decided so that the pole is placed at $-\omega_n$. Here, the plant is assumed to be the nominal plant as shown in Eq. (16).

The transfer function from n^* to n is expressed as Eq. (17) and is defined G_n.

$$\frac{n}{n^*} = \frac{\omega_n}{s+\omega_n} = G_n. \tag{17}$$

Therefore, K_p becomes as

$$K_p = 2\pi J_\omega K_p. \tag{18}$$

B. Designing of Lift Controller

In this part, the lift controller is designed and considered to be able to measure or estimate the lift of wing by calculating Eq. (10) and Eq. (13).

The controller is designed as a two-degree-of-freedom controller as shown in Fig. 4. C_F can be quadratically approximated using coefficients a_{CF}, b_{CF}, and c_{CF} as

$$C_F = a_{CF}J^2 + b_{CF}J + c_{CF}. \tag{19}$$

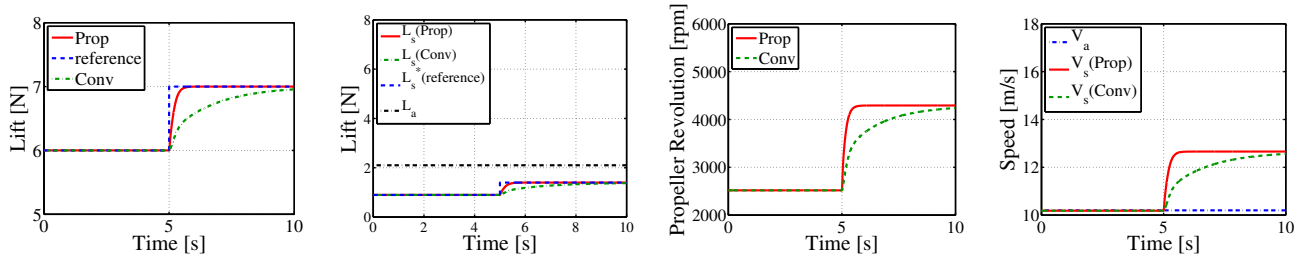

(a) Lift for all. (b) Lift of slipstream. (c) Propeller revolution. (d) Airspeed & Slipstream.

Fig. 7. Simulation results for step lift command.

From Eqs. (1), (8), and (19), L_s can be written as

$$L_s = \alpha_L n^2 + \beta_L n + \gamma_L, \tag{20}$$

where

$$\alpha_L = \frac{4}{\pi} C_L \rho S_s c_{CF} {D_p}^2,$$
$$\beta_L = \frac{4}{\pi} C_L \rho S_s D_p b_{CF} V_x,$$
$$\gamma_L = \frac{1}{2} C_L \rho S_s (\frac{8}{\pi} a_{CF} + 1) {V_x}^2.$$

Define function f as a function between revolution speed n and L_s as

$$L_s = f(n). \tag{21}$$

Feed forward controller C_{FF} is designed as follows. L_s is a function of the revolution speed reference n^* as

$$L_s = f(G_n \cdot n^*). \tag{22}$$

Therefore,

$$\begin{aligned} n^* &= {G_n}^{-1} \cdot f^{-1}(L_s) \\ &= \frac{s + \omega_{\mathrm{n}}}{\omega_{\mathrm{n}}} f^{-1}(L_s). \end{aligned} \tag{23}$$

Eq. (23) is non-proper, so feed forward controller C_{FF} is designed using reference model $G_g(s)$.

$$G_g(s) = \frac{\omega_g}{s + \omega_g}, \tag{24}$$

$$n^* = f^{-1}(L_s) \cdot {G_n}^{-1} \cdot G_g(s). \tag{25}$$

Here, ω_g is the pole of the reference model. Feed forward controller C_{FF} is a nonlinear variable controller as shown in Eq. (25), because $f^{-1}(L_s)$ varies by V_x and is non linear.

Next, feedback controller C_{I} is designed as follows. Feedback reference ${L_s}^*$ is created by multiplying reference model $G_g(s)$ to lift reference ${L_s}^*$ as ${L_{s_{\mathrm{FB}}}}^* = G_g(s){L_s}^*$ By using Taylor series at operating point $n = n_o$, $f(n)$ can be approximated to its first order.

$$L_s \approx (\alpha_L n_o + \beta_L)\, n + (\gamma_L - \alpha_L {n_o}^2). \tag{26}$$

The revolution speed controller is assumed to be fast enough so $n^* = n$. The feed back controller uses the difference of the reference and output, so when β_L is regard as a constant, Eq. (27) can be obtained as a transfer function G_L from n^* to L_s.

$$G_{\mathrm{L}} = \frac{\Delta L_s}{\Delta n^*} = \frac{\Delta L_s}{\Delta n} = \alpha_L n_o + \beta_L. \tag{27}$$

Lift control uses an integral controller, and the gain K_{I} is designed the placing the pole at $-\omega_{\mathrm{lift}}$ while the plant is assumed to be G_L.

$$\frac{L_s}{{L_s}^*} = \frac{\frac{K_{\mathrm{I}}(\alpha_L n_o + \beta_L)}{s}}{1 + \frac{K_{\mathrm{I}}(\alpha_L n_o + \beta_L)}{s}} = \frac{\omega_{\mathrm{lift}}}{s + \omega_{\mathrm{lift}}}. \tag{28}$$

Therefore, K_{I} becomes as

$$K_{\mathrm{I}} = \frac{\omega_{\mathrm{lift}}}{\alpha_L n_o + \beta_L}. \tag{29}$$

Here, K_{I} is function of n_{FF} and V_x, so lift feedback controller C_{I} is variable.

C. Controller Design Concept

In this part, controller design concept on this paper was explained. Assume that $N = 3$ propellers airplane shown in Fig. 5. 2 propellers on wing are controlled by the proposed method. A propeller on head is used for airspeed control[14] to keep airspeed constant by compensating thrust addition of the proposed method for future works.

ICE airplanes can only control propeller revolution speed. Accordingly, the conventional lift control method is set up as follows. Assume that pilot can give a revolution speed reference based on airspeed and lift reference feed forwardly without delay. The revolution speed control response speed is generally 2∼3 seconds. This time needs to be ensured to keep safely according to the inertia moment of the reciprocal engine and the setting time of the fuel-air ratio.

In the simulation and experiments of this paper, the revolution speed controller is a proportional and integral controller whose pole is ω_{conv} instead. The revolution speed reference is same as the proposed one.

IV. Simulation of Lift Control

Lift control method proposed in section III is verified by simulation.

A. Simulation Condition

The simulation model uses the parameter of APC10×10 E model propeller. The J–C_F and J–C_Q curves are shown in Fig. 6. The parameter including the airplane constants and the poles of each controller are as listed in Table. I.

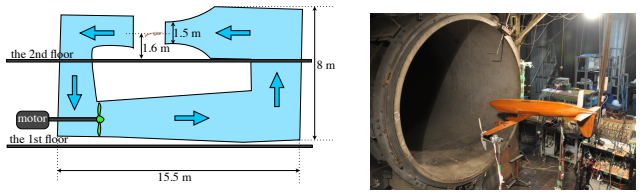

(a) Gettingen Wind tunnel diagram. (b) Experimental airplane.

Fig. 8. Wind tunnel overview.

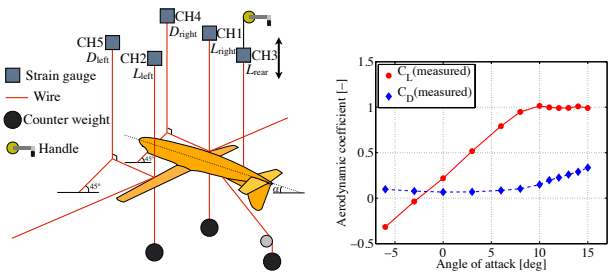

(a) Wire balance measuring method. (b) Model airplane lift and drag coefficient.

Fig. 9. Measuring aerodynamic.

B. Step Response Simulation

Step response simulation was conducted to the thrust controller. The airspeed was changed by the propeller thrust, and a step reference was given. When the airspeed V_x was set at $V_x = 10.0$ m/s, the simulation started at a steady state of lift $L_{\mathrm{all}} = 6.0$ N. At $t = 5.0$ s, lift reference changed from 6.0 N to 7.0 N.

The simulation result is shown in Fig. 7. Figure 7(a) is total lift L_{all} and Fig. 7(b) shows L_s and L_a of one side wing which are separated from L_{all}. The response is very fast for 0.2 s, because revolution speed response of the proposed method is quicker than that of conventional one in Fig. 7(c). Figure 7(d) shows the airspeed V_x and the propeller slipstream V_s which is depend on the propeller revolution.

From the comparison with the conventional method, the proposed one was verified to have quick and accurate response to the reference.

V. Experiment of Lift Control

In this section, lift control in use of propeller slipstream is verified by experiment.

A. Experimental Setup

The experimental units for this research are explained. Located in the aerospace engineering department at the University of Tokyo, one part of the units is a Goettingen type wind tunnel shown in Fig. 8(a) with a 1.5 m diameter of the opening. The wind tunnel reuse the wind which it generates, so there is less influence of the surrounding environment. The measuring of lift and drag is called 'wire balance method.' First, the airplane was supported by wires and the wires kept tension by counterweights as shown in Fig. 8(b). And then the wires were connected to strain gages to measure the difference tension as

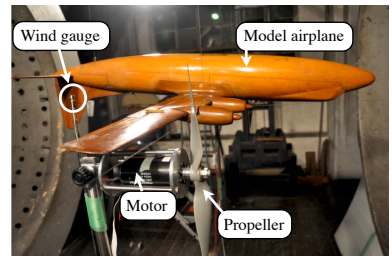

Fig. 10. Slipstream measuring equipment.

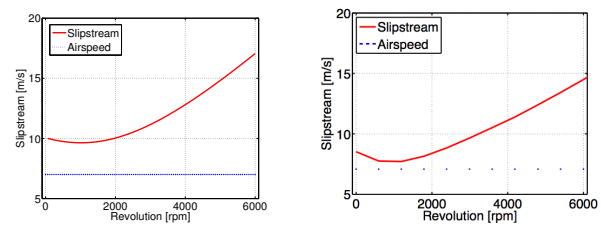

(a) Simulation. (b) Experiment.

Fig. 11. Slipstream measurement.

lift and drag. Lift and drag were calculated from Eq. (30) and Eq. (31).

$$L = L_{\mathrm{right}} + L_{\mathrm{left}} + L_{\mathrm{rear}}, \quad (30)$$

$$D = D_{\mathrm{right}} + D_{\mathrm{left}}. \quad (31)$$

Lift was occurred to upside of airplane, so the model airplane was supported to be upside down to keep wires tension. It is able to change the attack angle of airplane by moving the position of strain gage CH3.

The model airplane specification is same as the simulation in Table. I, and lift coefficient C_L and drag coefficient C_D were measured as shown in Fig. 9(b).

Two motors and two propellers are placed above the wing whose location is in propeller slipstream shown in Fig. 10. The motor mounts are able to adjustable angle of attack depending on the model plane attitude.

B. Measurement of Propeller Slipstream

In this part, propeller slipstream was measured in order to confirm the propeller slipstream theorem in Section II-B.

The propeller was rotated by a motor and the propeller slipstream was measured by an anemometer. Figure 11 showed the results about airspeed of wind tunnel and propeller slipstream depend on propeller revolution. Figure 11(a) is the simulation result and Fig. 11(b) is the experimental result. Between the simulation and the experiment, value was different, but the relationship between propeller revolution and slipstream was adjustable to theory.

C. Lift Control Experiment Results

In this part, in order to confirm the lift control proposed method, experiment was carried out. The airspeed was fixed and step reference was given.

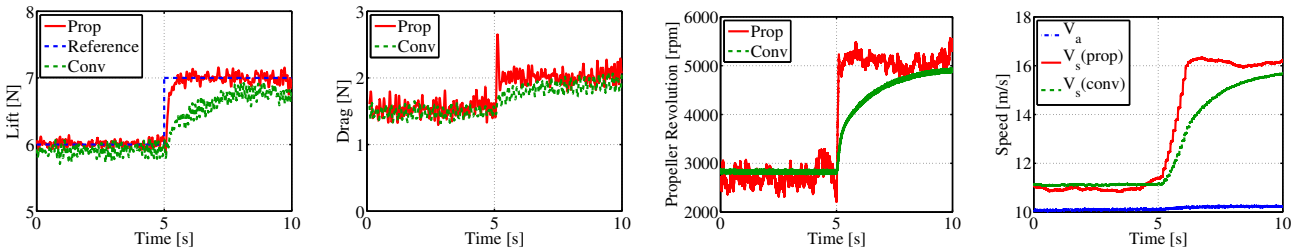

(a) Total lift. (b) Drag. (c) Revolution. (d) Airspeed.

Fig. 12. Lift control experiment results.

When the airspeed V_x was set at $V_x = 10$ m/s, the experiment started at lift reference $L_{\mathrm{all}} = 6.0$ N. At $t = 5.0$ s, lift reference changed from 6.0 N to 7.0 N.

The results were shown in Fig. 12. Figure 12(a) and Fig. 12(b) are the response of total lift and drag on wing, and Fig. 12(c) is the propeller revolution. At $t = 5.0$ s, propeller revolution was enlarged depend on step reference, and the slipstream was increased in Fig. 12(d). Compare to the conventional method, the response speed and accuracy was improved by the proposed method.

From considering scaling rule, 1.0 N increase for this experiment model airplane means 0.169 increase of lift coefficient C_L as non-dimensional value. If commercial airplanes adopt the proposal method, 800 N $\sim$ 5000 N will be increased as lift depending on airspeed. The effectiveness of the lift control by using propeller slipstream was confirmed from these results.

VI. Conclusion

This paper aimed at landing weight reduction by controlling the motors and propellers. In order to achieve the aim, the propeller slipstream was modeled and then used for the lift control. The reliability of the propeller slipstream theory was verified by experiments, and the effectiveness of the proposed method was verified by simulations and experiments.

The proposed method can improve the response speed and landing accuracy, compared to the conventional approaching and landing methods like powered lift system and flaring, and the method might be a key technology for landing assist in the future.

Future works include but not limit to: 1) further experiments of the lift control using wind tunnel, 2) design of a vertical velocity control without using the information of lift, 3) introducing an airspeed control approach into the proposed method of this paper by using extra propellers might be desirable.

Acknowledgment

This research was partly supported by the Ministry of Education, Culture, Sports, Science, and Technology grant (Basic Research A, number: 26249061).

References

[1] H. Kobayashi and A. Nishizawa: "Decrease in Ground-Run Distance of Airplanes by applying Electrically Driven Wheels," the 27th International Congress of the Aeronautical Sciences, 8 pages, (2010).

[2] G. Romeo, I. Moraglio, and C. Novarese: "ENFICA-FC: Preliminary Survey & Design of 2-Seat Aircraft Powered by Fuel Cells Electric Propusion," 7th AIAA Aviation Technology, Integration and Operations Conference, AIAA 2007-7754, 13 pages (2007).

[3] Tine Tomazic, Vid Plevnik, Gregor Veble, Jure Tomazic, Franc Popit, Saso Kolar, Radivoj Kikelj, Jacob W. Langelaan, and Kirk Miles: "Pipistrel Taurus G4: on Creation and Evolution of the Winning Aeroplane of NASA Green Flight Challenge 2011," Journal of Mechanical Engineering, Vol. 57, No. 12, pp. 869–878, (2011).

[4] M. D. Moore and Bill Fredericks: "Misconceptions of Electric Propulsion Aircraft and their Emergent Aviation Markets," the 52nd Aerospace Sciences Meeting AIAA SciTech, 17 pages (2014).

[5] Y. Hori: "Future Vehicle Driven by Electricity and Control-research on Four-Wheel-Motored UOT Electric March II," IEEE Trans. Ind. Electron, Vol. 51, No. 5, pp. 954–962, (2004).

[6] N. Konishi, H. Fujimoto, H. Kobayashi, and A. Nishizawa: "Range Extension Control System for Electric Airplane with Multiple Motors by Optimization of Thrust Distribution Considering Propellers Efficiency," 40th Annual Conference of the IEEE Industrial Electronics Society, pp. 2847–2852, (2014).

[7] A. M. Stall, J. B. Bevirt, M. D. Moore, J. Fredericks, and N. K. Borer: "Drag Reduction Through Distributed Electric Propulsion," 14th AIAA Aviation Technology, Integration and Operations Conference, pp. 16–20 (2014).

[8] International Business Aviation Council: "Business aviation safety brief Summary of Global Accident Statistics," International Business Aviation Council, No. 12, (2013).

[9] NASA Langley Research Center: "Powered Lift Aerodynamics and Acoustics," NASA-SP-406, (1976).

[10] S. Collins, B. Westra, and J. Lin,"Wind tunnel testing of powered lift, all-wing STOL model," 2008 International Powered Lift Conference, 11 pages, (2008).

[11] A. Vorobiev, R. M. Rennie, and E. J. Jumper: "Lift Enhancement by Plasma Actuators at Low Reynolds Numbers," Journal of Aircraft, Vol. 50, No. 1, pp. 12–19, (2013).

[12] Karl. H: "Aircraft Propeller Handbook," The Ronald Press Company, New York (1937).

[13] K. Takahashi, H. Fujimoto, Y. Hori, H. Kobayashi, and A. Nishizawa: "Modeling of Propeller Electric Airplane and Thrust Control using Advantage of Electric Motor," The 13th International Workshop on Advanced Motion Control, pp. 699–704 (2014).

[14] K. Takahashi, H. Fujimoto, Y. Hori, H. Kobayashi, and A. Nishizawa: "Airspeed Control of Electric Airplane Based on 2-Quadrant Thrust Control and Verification with Towing Test Using Electric Vehicle," 40th Annual Conference of the IEEE Industrial Electronics Society, pp. 2682–2688, (2014).